Thermodynamic properties of He-H_2 fluid mixtures over a wide range of temperatures and pressures

I. Ali,* S. M. Osman, N. Sulaiman, and R. N. Singh
Department of Physics, College of Science, Sultan Qaboos University, P. O. Box 36, Al-Khod 123, Oman
(Received 31 July 2003; revised manuscript received 1 December 2003; published 11 May 2004)

The effect of pressure P and temperature T on the properties of mixing of helium-hydrogen (He-H_2) fluid mixture is studied based on statistical mechanical perturbation theory. The constituent species are considered to be interacting via a pair potential consisting of short range repulsion and a long range attraction which has been included through a double Yukawa (DY) potential. He and H_2 are the lightest elements; therefore, the quantum effect is included via first-order quantum correction in the framework of Wigner-Kirkwood expansion. The dimerization of the H_2 molecule is treated as a hard convex body fluid for which the equation of state (EOS) can be derived from hard sphere system based on scaled particle theory. An advanced and most recent EOS has been used for our investigation. The use of the DY potential, which can readily be simulated to empirical potentials, has enabled us to obtain analytical expressions for attractive and quantum energy contributions in terms of Laplace transforms. With a view to ensure internal consistency of the various thermodynamic functions to extract information on segregation and order in the mixture, different functions, such as compressibility factor, Gibbs free energy of mixing, entropy of mixing, and concentration fluctuations in the long wavelength limit, have been calculated as functions of composition of the mixture over an extended region of P and T. The results suggest that segregation, heterocoordination, or both may occur in the He-H_2 mixture depending upon its composition, pressure, and temperature.

DOI: 10.1103/PhysRevE.69.056104 PACS number(s): 05.70.−a, 65.20.+w

I. INTRODUCTION

The problem of mutual solubility as a function of composition, temperature, and pressure in a mixture is extremely useful either to design a separation equipment or to synthesize a homogeneous phase. Conditions involving extreme temperature T and pressure P are also useful to investigate condensed explosions. At extreme T and P a direct measurement is not feasible due to unfavorable experimental conditions. Therefore, a theoretical approach based on the theory of mixture is very much needed provided the effects of T and P are rightfully incorporated in the formalism. The present work is an attempt in this direction with an application to study the solubility of He and H_2 at low T and elevated P.

The helium-hydrogen (He-H_2) system derives special attention because the mixture carries enormous significance [1–3] from both theoretical and cosmological points of view. The component species are known to exhibit characteristic phenomena at extreme P and T, whereas the mixture exhibits fluid-fluid phase separation up to very high pressures. Both He and H_2 have complex attractive and repulsive interactions [4]. Therefore, the forces between unlike molecules in the mixture play significant [5,6] roles on its properties. Also, the masses are light making quantum effects important at low temperatures.

We consider here the statistical mechanical perturbation theory [7] of a binary hard sphere mixture with necessary correction for attractive forces and quantum effects. The approach is versatile and has been used successfully to construct the phase diagram of a binary mixture of hard core molecules with square wells. Comparison with Refs. [8,9] and computer simulation results [10] shows that the scheme is as good as, or even better than, other mixture theories, such as the Percus-Yevick theory. One of the foremost advantages is that the hard sphere diameter can be made dependent on temperature and, hence, the solubility of He-H_2 mixture can be investigated over a wide range of temperature and pressure.

The short range repulsive potential is treated here as the unperturbed reference system of the hard sphere mixture which is appropriately improved through a first-order perturbation contribution due to long range attractive potential. The latter is treated within the framework of the double Yukawa (DY) potential. There is ample evidence in the literature [11–13] that the DY potential provides accurate thermodynamic properties of fluids. The advantage of using the DY potential is that it gives analytical expressions for the Helmholtz free energy and hence for other thermodynamic functions. We will see that the DY potential can readily be parametrized to simulate the exponential-6 potential, which has been used by Ree [5] to perform the Monte Carlo calculations on He-H_2 mixture, yielding a satisfactory result over extended density and temperatures ranges.

The quantum effect is included via a first-order quantum correction in the Wigner-Kirkwood expansion [14,15]. The dimerization of H_2 molecule is treated as a hard convex body (HB) fluid for which an equation of state can be derived based on scaled particle theory [16,17]. Taking into account the various contributions, we have been able to suggest an improved version of the equation of state to study the compressibility factor Z, the excess Gibbs free energy G_{xs}, the excess entropy S_{xs}, and the concentration fluctuations $S_{cc}(0)$, in the long wavelength limit. These are used to investigate

*Corresponding author: Email address: issam@squ.edu.om

the effects of P and T on the thermodynamic properties of He-H_2 mixture over a wide range of densities and composition. The major thrust is to examine the deviation of the He-H_2 mixture from the ideal mixing conditions to investigate the heterocoordination or segregation (phase separation) of the mixture.

The equation of state of He-H_2 system, duly improved for long range correlations and quantum effects, is derived in Sec. II. Yukawa potentials for the component interactions (H_2-H_2, He-He, and He-H_2) are obtained. The computed values of Z in the low and high density regions, the impact of P and T, and the role of the radial distribution function are discussed in Sec. III. Expressions for the Gibbs free energy are given in Sec. IV. These expressions are used to compute the excess free energy over a wide range of P and T. Section V deals with excess entropy of mixing. Concentration fluctuations and the thermodynamic stability are discussed in Sec. VI. We then follow with Sec. VII, dealing with summary and conclusions.

II. PAIRWISE INTERACTIONS AND EQUATION OF STATE OF He-H_2 MIXTURE

A. Potentials for the He-H_2 system

The equation of state (EOS) of the He-H_2 mixture, which will be obtained here on the basis of statistical mechanical perturbation theory, is at the center of our investigation. Our major improvement in writing the EOS concerns the inclusion of long range correlations and quantum correction for the energy, which, in turn, depend on the interaction potential and the distribution functions. The constituent elements are assumed to be interacting via a pair potential $u_{ij}(r)$ consisting of short range repulsion $u_{ij}^{\mathrm{HS}}(r)$ (usually the hard sphere potential) and a long range attraction $u_{ij}^{\mathrm{t}}(r)$,

$$u_{ij}(r) = u_{ij}^{\mathrm{HS}}(r) + u_{ij}^{\mathrm{t}}(r). \tag{1}$$

$u_{ij}^{\mathrm{HS}}(r)$ is treated as the unperturbed reference system on which $u_{ij}^{\mathrm{t}}(r)$ acts as a perturbation. The long range attraction forces have been included through the DY potential, given by

$$u_{ij}^{\mathrm{DY}}(r) = \epsilon_{ij} A_{ij} \frac{\sigma_{ij}^0}{r} \left\{ \exp\left[-\lambda_{ij}\left(\frac{r}{\sigma_{ij}^0} - 1 \right) \right] - \exp\left[-\nu_{ij}\left(\frac{r}{\sigma_{ij}^0} - 1 \right) \right] \right\}. \tag{2}$$

ϵ_{ij} represent the strengths of potential minima and σ_{ij}^0 the value of r at which the potential is effectively zero. A_{ij}, λ_{ij}, and ν_{ij} are controlling parameters of the potential. The advantage of using the DY potential is that the related integral equation of the Helmholtz free energy and, hence, the compressibility factor can be solved analytically. The parameters can be chosen to reproduce the various available empirical potentials which are often used in simulation work.

Ree [5] performed Monte Carlo simulations on the He-H_2 mixture with exponential-6 (exp-6) potential and found it satisfactory over an extended range of density and temperature, where the other conventional model is physically less appropriate. *Ab initio* quantum mechanical calculations and the analysis of data on He and H_2 conform to the choice of the exp-6 potential. We have, therefore, simulated our DY potential to Ree's [5] exp-6 potential. The emerging parameters for DY potential are given in Table I.

TABLE I. DY potential parameters for He-He, H_2-H_2, and He-H_2 pairwise interactions. Exp-6 potentials (Ree [5]) have been used to fit the DY parameters.

	He-He	H_2-H_2	He-H_2
i,j	1,1	2,2	1,2
σ_{ij}^0 (Å)	2.63	2.98	2.97
ϵ_{ij}/k (K)	10.57	36.4	15.5
A_{ij}	2.548	3.179	2.801
λ_{ij}	12.204	9.083	10.954
ν_{ij}	3.336	3.211	3.386

The intermolecular or interatomic force is a fundamental issue to study the properties of matter. It has always been a subject of great interest to determine the forces between unlike molecules from the knowledge of the forces between the like molecules. In the absence of reference potentials, the parameters ϵ_{ij}, A_{ij}, λ_{ij}, ν_{ij}, and σ_{ij}^0 are considered additive [$\epsilon_{12}=\sqrt{\epsilon_{11}\epsilon_{22}}$; $A_{12}=(A_{11}+A_{22})/2$; $\lambda_{12}=(\lambda_{11}+\lambda_{22})/2$; $\nu_{12}=(\nu_{11}+\nu_{22})/2$; $\sigma_{12}^0=(\sigma_{11}^0+\sigma_{22}^0)/2$] as per the Lorentz-Berthelot rule of mixing. However, with reference to Ree's [5] exp-6 potentials, we observe that these parameters are close to the additive rule, but ϵ_{12} deviates considerably. The nonadditive energy parameter ϵ_{12} is described in terms of the factor α, i.e.,

$$\epsilon_{12} = \alpha\sqrt{\epsilon_{11}\epsilon_{22}}. \tag{3}$$

α signifies the relative strength of the unlike pairwise interactions in the mixture. The data of Table I suggest that $\alpha = 0.79$. The role of α in probing phase separation and compound formation in binary mixtures, in general, has been discussed at length by Osman and Singh [18,19].

B. Equation of state

The elemental components, He and H_2, are treated as monomers and dimers, respectively. The complexities of the intermolecular interactions and the geometrical shapes of dimers make it difficult to use theoretical models to investigate the properties of mixing of monomer-dimer binary mixtures. There are many real monomer-dimer systems, including He-H_2 mixtures, which are of considerable significance for practical applications. Good progress has been made in recent years to develop a realistic equation of state EOS for nonspherical hard body fluids such as hard convex body HB fluids [16,17].

The major limitation to the EOS of HB fluids is that it does not incorporate the contribution from the long range correlations and the quantum effects of energy which are important for systems such as He-H_2. Taking into account the quantum term and the contribution to the EOS from long range correlations, the compressibility factor Z ($=P/\rho kT$, ρ is

density and k is Boltzmann constant) can be expressed, to first-order statistical mechanical perturbation theory, as

$$Z = Z^{\mathrm{HB}} + Z^{\mathrm{t}} + Z^{\mathrm{Q}}. \tag{4}$$

Z^{HB} is the compressibility factor of HB (hard body) fluid mixture, Z^{t} arises due to long range correlations, and Z^{Q} incorporates the first-order quantum correction, which is quite significant in the lower temperature region. An expression for Z^{HB} has been developed based on the scaled particle theory [16,17]. It can be expressed in terms of the EOS of hard sphere mixture (HS) through the nonsphericity parameter a_{mix},

$$Z^{\mathrm{HB}} = 1 + a_{\mathrm{mix}}(Z^{\mathrm{HS}} + Z^{\mathrm{nonadd}} - 1), \tag{5}$$

where Z^{HS} is the compressibility factor of an additive HS system. The correction term, Z^{nonadd}, arises [7] due to nonadditivity. Boublik [20] and Mansoori *et al.* [21] (denoted here by BMCSL) have suggested an improved version of the EOS for additive HS. Barrio and Solana [22] used the consistency conditions to improve the contact values of the pair correlation function and suggested a correction term Z^{BS} to the EOS of BMCSL. This satisfies the thermodynamic consistency conditions vis-à-vis standardized fourth and fifth virial coefficients. With these improvements, Z^{HS} can be expressed as

$$Z^{\mathrm{HS}} = Z^{\mathrm{BMCSL}} + Z^{\mathrm{BS}}, \tag{6}$$

with

$$Z^{\mathrm{BMCSL}} = \frac{1}{(1-\eta_3)} + \frac{3\eta_1\eta_2}{\eta_0(1-\eta_3)^2} + \frac{\eta_2^3(3-\eta_3)}{\eta_0(1-\eta_3)^3} \tag{7}$$

and

$$Z^{\mathrm{BS}} = \frac{\eta_1\eta_2(\eta_4 z_1 + \eta_0 z_2)}{(1-\eta_3)^2}. \tag{8}$$

η_i and z_i stand for

$$\eta_i = \frac{\pi}{6}\rho(c_1\sigma_{11}^i + c_2\sigma_{22}^i),$$

$$z_1 = 2c_1c_2\sigma_{11}\sigma_{22}\left(\frac{\sigma_{11}-\sigma_{22}}{\sigma_{11}+\sigma_{22}}\right), \tag{9}$$

$$z_2 = c_1c_2\sigma_{11}\sigma_{22}^3(\sigma_{11}^2 - \sigma_{22}^2).$$

c_i $(=\rho_i/\rho)$ are mole fractions and σ_{ii} are hard sphere diameters of the component i. For a one-component system (pure fluid), $\sigma_{11}=\sigma_{22}=\sigma$, $Z^{\mathrm{BS}}\to 0$, and Z^{HS} reduces to the Carnahan-Starling (CS) [23] EOS,

$$Z^{\mathrm{HS}} = Z^{\mathrm{CS}} = \frac{1+\eta+\eta^2-\eta^3}{(1-\eta)^3}, \tag{10}$$

where $\eta = \pi\rho\sigma^3/6$ is the packing fraction.

a_{mix} in Eq. (5) is the nonsphericity parameter for the scaling theory [24],

$$a_{\mathrm{mix}} = \frac{1}{V_{\mathrm{mix}}}\sum_{ij} c_i c_j V_{ij}^{\mathrm{ef}} a_{ij}^{\mathrm{ef}}, \tag{11}$$

with

$$V_{\mathrm{mix}} = \sum_{ij} c_i c_j V_{ij}^{\mathrm{ef}}. \tag{12}$$

The parameters V_{ij}^{ef} and a_{ij}^{ef} are related to the average molecular volume and the shape factor of a mixture dimer molecule, respectively,

$$V_{ij}^{\mathrm{ef}} = \frac{\pi}{6}\sigma_{ii}^3\overline{V}_{ij}, \tag{13}$$

$$a_{ij}^{\mathrm{ef}} = \frac{1}{3\pi}\frac{(V_{ij}^{\mathrm{ef}})'(V_{ij}^{\mathrm{ef}})''}{V_{ij}^{\mathrm{ef}}}, \tag{14}$$

where

$$\overline{V}_{ij} = 1 + (n_i - 1)\left[\frac{3}{2}\left(1 + \frac{\sigma_{jj}^2}{\sigma_{ii}^2}\right)L_i - \frac{1}{2}L_i^3 - 3H_{ij}\theta_{ij}\left(\frac{\sigma_{jj}}{\sigma_{ii}}\right)^2\right]. \tag{15}$$

$\overline{V}_{ij}$ is the volume factor for the average molecular volume, n_i is the number of elemental spheres ($n_i=2$ for H_2), each with diameter σ_{ii} and center to center diameter l_i in the molecule [17], and

$$H_{ij} = \frac{1}{2\sigma_{ii}}[(\sigma_{ii}+\sigma_{jj})^2 - l_i^2]^{1/2},$$

$$\theta_{ij} = \sin^{-1}\left[\frac{l_i}{\sigma_{ii}+\sigma_{jj}}\right],$$

$$L_i = \frac{l_i}{\sigma_{ii}}. \tag{16}$$

$(')$ and $('')$ in Eq. (14) refer to the first and second derivatives, respectively, with respect to σ_{ij}, i.e.,

$$(V_{ij}^{\mathrm{ef}})' = \left(\frac{\partial V_{ij}^{\mathrm{ef}}}{\partial \sigma_{ii}}\right)_{\sigma_{jj}} + \left(\frac{\partial V_{ij}^{\mathrm{ef}}}{\partial \sigma_{jj}}\right)_{\sigma_{ii}}, \tag{17}$$

$$(V_{ij}^{\mathrm{ef}})'' = \left(\frac{\partial^2 V_{ij}^{\mathrm{ef}}}{\partial \sigma_{ii}^2}\right)_{\sigma_{jj}} + 2\frac{\partial^2 V_{ij}^{\mathrm{ef}}}{\partial \sigma_{ii}\,\partial \sigma_{jj}} + \left(\frac{\partial^2 V_{ij}^{\mathrm{ef}}}{\partial \sigma_{jj}^2}\right)_{\sigma_{ii}}. \tag{18}$$

For monomers $(n\to 1)$, $V^{\mathrm{ef}}=V=\pi\sigma^3/6$ and $a_{\mathrm{mix}}=1$, hence, the compressibility factor in Eq. (5) reduces to that of hard spheres ($Z^{\mathrm{HB}}\to Z^{\mathrm{HS}}$).

Z^{nonadd} in Eq. (5) is the correction term arising due to nonadditivity $[(\sigma_{11}+\sigma_{22})/2 \neq \sigma_{12}]$ of the hard sphere diameters. Leonard *et al.* [7] have used the first-order statistical mechanical perturbation theory to obtain an expression for the Helmholtz free energy F^{nonadd} [see Sec. IV, Eq. (43)] due to nonadditivity. We have used it to obtain an expression for Z^{nonadd} through the thermodynamic relation

$$Z = \rho\left(\frac{\partial \beta F}{\partial \rho}\right)_{c,T}, \tag{19}$$

where $\beta = 1/kT$. This gives

$$Z^{\text{nonadd}} = -4\pi\rho c_1 c_2 \bar{\sigma}_{12}^2 \Delta\sigma_{12}\left[g_{12}^{\text{HS}}(\sigma_{12}) - \rho\left(\frac{\partial g_{12}^{\text{HS}}(\sigma_{12})}{\partial \rho}\right)_c\right], \tag{20}$$

with

$$\bar{\sigma}_{12} = \frac{\sigma_{11} + \sigma_{22}}{2} \quad \text{and} \quad \Delta\sigma_{12} = \bar{\sigma}_{12} - \sigma_{12}. \tag{21}$$

σ_{ij} have been calculated using the integral equation [7]

$$\sigma_{ij} = \int_0^{\sigma_{ij}^0} \{1 - \exp[-\beta u_{ij}(r)]\} dr. \tag{22}$$

Equation (22) relates σ_{ij} to the pairwise interaction potential $u_{ij}(r)$ for which we use $u_{ij}^{\text{DY}}(r)$ in Eq. (2). We may recall that σ_{ij} determine the static structure factors and, therefore, a suitable link between structure and forces has been established. Further, Eq. (22) allows σ_{ij} to be temperature dependent, which is desirable on a more realistic basis to examine the mixing and demixing of mixtures as functions of T. Osman and Singh [19] have discussed at length the T dependence of σ_{ij} emerging from Eq. (22) for a Lennard-Jones system.

$g_{12}^{\text{HS}}(\sigma_{12})$ in Eq. (20) refers to the radial distribution function (RDF) at $r = \sigma_{12}$, the contact point. It has been emphasized [25,26] that the inclusion of contact values improves the performance of the RDF and yields exact asymptotic expressions for the thermodynamic properties. Based on the consistency conditions of these properties, Barrio and Solana [22] improved the existing BMCSL expression as

$$g_{12}^{\text{HS}}(\sigma_{12}) = g_{12}^{\text{BMCSL}}(\sigma_{12}) + g_{12}^{\text{BS}}(\sigma_{12}), \tag{23}$$

with

$$g_{12}^{\text{BMCSL}}(\sigma_{12}) = \frac{1}{1-\eta_3} + \frac{3D\eta_2}{(1-\eta_3)^2} + \frac{2D^2\eta_2^2}{(1-\eta_3)^3},$$

$$g_{12}^{\text{BS}}(\sigma_{12}) = \frac{\sigma_{11}\sigma_{22}^3(\sigma_{11} - \sigma_{22})}{4\sigma_{12}^2}\frac{\eta_1\eta_2}{(1-\eta_3)^2},$$

$$D = \frac{\sigma_{11}\sigma_{22}}{2\bar{\sigma}_{12}}. \tag{24}$$

D is the reduced collision parameter. The derivative, $\partial g_{12}^{\text{HS}}(\sigma_{12})/\partial\rho$, can readily be obtained from the above relations.

The expressions for Z^{t} and Z^{Q} are obtained from F^{t} and F^{Q} [see Eqs. (45) and (47), Sec. IV] through Eq. (19). The resulting expressions are

$$Z^{\text{t}} = \frac{2\pi\rho^*}{T^*}[c_1^2(k_{11} + \rho^* k'_{11}) + 2c_1c_2\alpha\sqrt{\bar{\epsilon}\bar{\gamma}}(k_{12} + \rho^* k'_{12}) + c_2^2\bar{\epsilon}\bar{\gamma}(k_{22} + \rho^* k'_{22})], \tag{25}$$

$$Z^{\text{Q}} = \frac{\pi Q\rho^*}{6T^*}\left[c_1^2(L_{11} + \rho^* L'_{11}) + \frac{2c_1c_2\alpha\sqrt{\bar{\epsilon}}}{\bar{\gamma}\bar{\Delta}}(L_{12} + \rho^* L'_{12}) + \frac{c_2^2\bar{\epsilon}}{\gamma\Delta}(L_{22} + \rho^* L'_{22})\right], \tag{26}$$

with

$$\rho^* = \rho\sigma_{11}^{03}, \quad \gamma = \frac{\sigma_{22}^0}{\sigma_{11}^0}, \quad \bar{\gamma} = \frac{\sigma_{12}^0}{\sigma_{11}^0}, \quad T^* = \frac{kT}{\epsilon_{11}}, \quad \bar{\epsilon} = \frac{\epsilon_{22}}{\epsilon_{11}},$$

$$\Delta = \frac{m_{22}}{m_{11}}, \quad \bar{\Delta} = \frac{m_{12}}{m_{11}}, \quad m_{12} = c_1m_1 + c_2m_2,$$

and

$$Q = \frac{N_A h^2}{4\pi^2\epsilon_{11}^0 m_{11}\sigma_{11}^{02}}. \tag{27}$$

h is Planck's constant, N_A is Avogadro's number, and m_{ij} are the atomic masses. The coefficients k_{ij}, k'_{ij}, L_{ij}, and L'_{ij} in Eqs. (25) and (26) involve the Laplace transforms of the RDF and are defined as

$$k_{ij} = \bar{V}_{ij}A_{ij}[e^{\lambda_{ij}}G_{ij}(\bar{\lambda}_{ij}) - e^{\nu_{ij}}G_{ij}(\bar{\nu}_{ij})],$$

$$k'_{ij} = \bar{V}_{ij}A_{ij}\left[e^{\lambda_{ij}}\frac{\partial G_{ij}(\bar{\lambda}_{ij})}{\partial\rho} - e^{\nu_{ij}}\frac{\partial G_{ij}(\bar{\nu}_{ij})}{\partial\rho}\right],$$

$$L_{ij} = \bar{V}_{ij}A_{ij}[\lambda_{ij}^2 e^{\lambda_{ij}}G_{ij}(\bar{\lambda}_{ij}) - \nu_{ij}^2 e^{\nu_{ij}}G_{ij}(\bar{\nu}_{ij})],$$

$$L'_{ij} = \bar{V}_{ij}A_{ij}\left[\lambda_{ij}^2 e^{\lambda_{ij}}\frac{\partial G_{ij}(\bar{\lambda}_{ij})}{\partial\rho} - \nu_{ij}^2 e^{\nu_{ij}}\frac{\partial G_{ij}(\bar{\nu}_{ij})}{\partial\rho}\right], \tag{28}$$

where

$$\bar{\lambda}_{11} = \lambda_{11}, \quad \bar{\nu}_{11} = \nu_{11}, \quad \bar{\lambda}_{22} = \frac{\lambda_{22}}{\gamma}, \quad \bar{\nu}_{22} = \frac{\nu_{22}}{\gamma},$$

$$\bar{\lambda}_{12} = \frac{\lambda_{12}}{\bar{\gamma}}, \quad \bar{\nu}_{12} = \frac{\nu_{12}}{\bar{\gamma}}. \tag{29}$$

The values of the Yukawa potential parameters A_{ij}, λ_{ij}, ν_{ij}, and ϵ_{ij} for the He-H_2 system are listed in Table I. $G_{ij}(\lambda_{ij})$ are the Laplace transforms of the RDF,

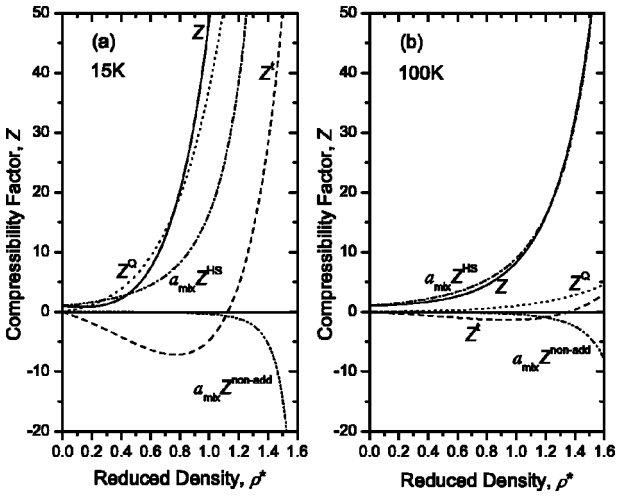

FIG. 1. Various terms of the compressibility factors (Z^{HB}, Z^{nonadd}, Z^{t}, and Z^{Q}) vs ρ^* ($=\rho\sigma_{11}^3$) for equiatomic ($c_{He}=c_{H_2}=0.5$) He-H_2 mixture: (a) $T=15$ K, (b) $T=100$ K.

$$G_{ij}(\overline{\lambda_{ij}}) = \int_{\sigma_{ij}}^{\infty} r g_{ij}^{HS}(r)\exp(-\overline{\lambda_{ij}}r)dr. \tag{30}$$

Similar expressions exist for $G_{ij}(\overline{\nu_{ij}})$. Following the work of Tang and Lu [27], the expressions for $G_{ij}(\overline{\lambda_{ij}})$ can be found analytically.

III. COMPRESSIBILITY FACTOR

It is evident from the preceding section that density ρ plays a vital role in the evaluation of compressibility factor Z. At low densities Z tends to its ideal value of 1. For example, as $\rho\to 0$ then $Z^{t}\to 0$, $Z^{Q}\to 0$, $Z^{nonadd}\to 0$, $Z^{HB}\to 1$ and, therefore, from Eq. (4) one has $Z\to 1$. On the other hand, at very high densities, Z increases sharply with ρ. All terms (Z^{HB}, Z^{Q}, Z^{t}, and Z^{nonadd}) tend to infinity as $\rho\to\infty$.

The variation of the various terms of Z for He-H_2 mixture at equiatomic composition ($c_{He}=c_{H_2}=0.5$) with respect to reduced density ρ^* at 15 K and 100 K is shown in Figs. 1(a) and 1(b), respectively. The required inputs are taken from Table I. The various components of Z, as well as its gradient $\partial Z/\partial\rho^*$, depend strongly on density in the lower temperature range ($T\sim 15$ K). Z^{HB} and Z^{Q} are positive at all densities with Z^{Q} being the most significant contribution at low temperature. For densities $\rho^*\leqslant 1.1$, Z^{t} contributes negatively and then rises sharply to positive values as density increases. The contribution of the nonadditive hard sphere term Z^{nonadd} is negligible for $\rho^*<1.0$, in comparison with other contributions, but decreases sharply as density increases. At $T=100$ K, however, the main contribution to Z arises from Z^{HB}. The impact of all other contributions (Z^{Q}, Z^{t}, and Z^{nonadd}) is small [Fig. 1(b)] in comparison to Z^{HS}.

With regard to the impact of the distribution function $g_{ij}^{HS}(r)$, it enters directly into the expressions of Z^{t} and Z^{Q}, through energy equation [see Eqs. (44) and (46)] and, hence, affects Z. From the viewpoint of mathematical simplicity, it is often preferred to perform the integral equations of the free energy analytically in the dilute limit, $g_{ij}(r,\sigma_{ij},\rho)\to 1$. This simplifies Z^{t} and Z^{Q} considerably, at the cost of a realistic $g(r)$. We found that Z calculated from hard sphere values of $g_{ij}^{HS}(r)$ is larger than that calculated from the condition $g_{ij}(r)=1$. At low temperature ($T\sim 15$ K), $g(r)$ influences Z considerably, being maximum towards the high density region. The impact of realistic $g(r)$ on Z at high temperature ($T=100$ K) is quite minimal. It can be inferred that $g(r)=1$ for He-H_2 system can be appropriate only at high temperatures.

We have compared in Table II our theoretical values of the pressure and the excess internal energy to the Monte Carlo simulation results [5] of He-H_2 mixture at different compositions and temperatures. Ree [5] performed Monte Carlo (MC) simulations on the He-H_2 mixture as a van der Waals one-fluid model for exp-6 potential. The stiffness of the intermolecular repulsion of the different constituent species was included. The MC results were recommended to be "exact" and quite appropriate for the thermodynamic investigations for extended regions of T and P. Theoretical values of P have been obtained from the respective compressibility factor contributions, i.e., $P=\rho kT(Z^{HB}+Z^{t}+Z^{Q})$. The com-

TABLE II. Comparison of pressure P and excess internal energy E^{xs} from this study to MC results [5], P_{MC} and E_{MC}^{xs}, for He-H_2 mixture at different temperatures T and He compositions c_{He}. The corresponding reduced density ρ^* and packing fraction η are also listed.

T (K)	c_{He}	ρ^*	η	P_{MC} [5] (GPa)	P (this study) (GPa)	E_{MC}^{xs} [5] (kJ mol^{-1})	E^{xs} (this study) (kJ mol^{-1})
50	0.50	0.550	0.265	0.0473	0.0491	−0.755	−0.593
100	0.50	0.786	0.346	0.3380	0.2570	−0.354	−0.466
300	0.25	1.101	0.433	2.3090	1.9664	2.790	2.741
300	0.50	1.101	0.400	1.8560	1.5729	3.490	2.166
300	0.75	1.101	0.367	1.4240	1.3160	2.008	1.737
1000	0.25	1.223	0.363	5.2250	4.8622	8.860	10.416
1000	0.50	1.223	0.335	4.5100	4.1094	10.88	8.315
1000	0.75	1.223	0.307	3.7150	3.5904	6.790	6.474
4000	0.50	1.376	0.247	12.4300	12.1014	25.120	24.871
4000	0.50	1.572	0.282	16.3300	16.4720	31.400	32.832

puted values are in reasonable agreement with MC results over a wide range of T and P. This suggests that our formalism of equation of state for He-H_2 mixture is quite good and can be used to derive and investigate other thermodynamic functions, such as Gibbs free energy of mixing, entropy of mixing, and concentration fluctuations in the long wavelength limit as functions of compositions c, T, and P, which we obtain in the following sections.

IV. GIBBS FREE ENERGY OF MIXING

Gibbs energy of mixing, G_M, plays a vital role in determining the thermodynamic stability of the phases in a binary mixture. It is convenient to describe the thermodynamic behavior in terms of the excess free energy of mixing, G_{xs}, defined as

$$G_{xs} = G_M - NkT\sum_i c_i \ln c_i, \tag{31}$$

with

$$G_M = G - \sum_i c_i G_i^0. \tag{32}$$

G is the Gibbs free energy of the mixture and $G_i^0 = G(c_i \rightarrow 1)$ are the free energies of the constituent species. An explicit expression for G can be written in terms of the Helmholtz free energy F and the pressure P,

$$\frac{G}{NkT} = \frac{F}{NkT} + \frac{P}{\rho kT}. \tag{33}$$

Having defined the compressibility factor Z in Eq. (4), it is now possible to obtain an analytical expression for the Helmholtz free energy F from the integral equation

$$\frac{F^{xs}}{NkT} = \int_0^\rho (Z-1)\frac{d\rho}{\rho}. \tag{34}$$

F^{xs} stands for the excess Helmholtz free energy. In conformity with Eq. (4), F for the mixture can be written as

$$\frac{F}{N} = F^{id} + F^{HB} + F^{t} + F^{Q}. \tag{35}$$

The subscripts carry the same meaning as in Eq. (4). The extra term F^{id} arises due to the ideal gas mixture term, i.e.,

$$\beta F^{id} = \frac{3}{2}\ln\left(\frac{h^2}{2\pi kT m_{11}^{c_1} m_{22}^{c_2}}\right) + \ln\rho + \sum_i c_i \ln c_i - 1. \tag{36}$$

The Helmholtz free energy F^{HB} for hard convex body becomes

$$\beta F^{HB} = a_{mix}\beta(F^{HS} + F^{nonadd}), \tag{37}$$

where a_{mix} is defined in Eq. (11). Equations (6) and (34) yield

$$\beta F^{HS} = \frac{\eta_3[f_1 + (2-\eta_3)f_2]}{(1-\eta_3)} + \frac{\eta_3 f_3}{(1-\eta_3)^2} + (f_3 + 2f_2 - 1)\ln(1-\eta_3), \tag{38}$$

with

$$f_1 = \frac{3y_1y_2}{y_0y_3}, \tag{39}$$

$$f_2 = \frac{y_1y_2}{y_3^2}(y_4z_1 + y_0z_2), \tag{40}$$

$$f_3 = \frac{y_2^3}{y_0y_3^3}, \tag{41}$$

$$y_i = \frac{\eta_i}{\rho} = \frac{\pi}{6}(c_1\sigma_{11}^i + c_2\sigma_{22}^i). \tag{42}$$

The contribution F^{nonadd}, which arises by the virtue of nonadditivity of the hard sphere diameters, is the first-order perturbation correction [7],

$$\beta F^{nonadd} = -4\pi\rho c_1c_2\overline{\sigma}_{12}^2\Delta\sigma_{12}g_{12}^{HS}(\sigma_{12}). \tag{43}$$

$\overline{\sigma}_{12}$ and $\Delta\sigma_{12}$ are defined in Eq. (21). The expression for the radial distribution function $g_{12}^{HS}(\sigma_{12})$ is given in Eq. (23).

F^t, in Eq. (35), which is the first-order perturbation contribution due to long range attractions, is of considerable significance. We have used the statistical mechanical theory to evaluate F^t from the integral equations containing the distribution functions $g_{ij}(r)$ and $u_{ij}(r)$, i.e.,

$$\beta F^t = \beta\frac{\rho}{2}\sum_{ij} c_ic_j\int_{\sigma_{ij}^0}^\infty u_{ij}^{DY}(r)g_{ij}^{HS}(r,\sigma_{ij},\rho)4\pi r^2\overline{V}_{ij}\,dr. \tag{44}$$

The integral above has been obtained analytically for $u_{ij}(r)$ given in Eq. (2) using the BMCSL [20,21] expression for $g_{ij}^{HS}(r)$; we obtain

$$\beta F^t = \frac{2\pi\rho^*}{T^*}[c_1^2k_{11} + 2c_1c_2k_{12}\alpha\sqrt{\overline{\epsilon\gamma}} + c_2^2k_{22}\gamma\overline{\epsilon}]. \tag{45}$$

ρ^* and T^* are defined in Eq. (27) and the coefficients k_{ij} in Eq. (28).

The last term, F^Q, in Eq. (35) is the first-order quantum correction to the free energy. The Wigner-Kirkwood [14,15] expansion for a one-component fluid can be conveniently generalized to a binary mixture as

$$\beta F^Q = \frac{h^2\beta^2N\rho^*}{96\pi^2}\sum_{ij}\frac{c_ic_j}{m_{ij}}\int_{\sigma_{ij}}^\infty \nabla^2u_{ij}(r)g_{ij}^{HS}(r)4\pi r^2\overline{V}_{ij}\,dr. \tag{46}$$

On using the double Yukawa potential from Eq. (2) for $u_{ij}(r)$ and carrying out the Laplacian operator one gets

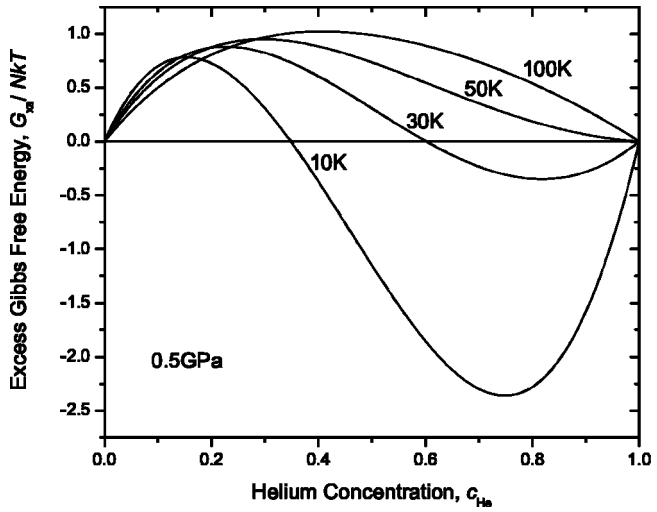

FIG. 2. Effect of temperature (T=10 K, 30 K, 50 K, and 100 K) on excess Gibbs free energy (G_{xs}/NkT) at P=0.5 GPa for He-H_2 mixture as a function of helium concentration c_{He}.

$$\beta F^{Q} = \frac{\pi Q \rho^{*}}{6T^{*2}}\left[c_1^2 L_{11} + \frac{2c_1 c_2 \alpha\sqrt{\bar{\epsilon}}}{\bar{\gamma}\bar{\Delta}} L_{12} + \frac{c_2^2 \bar{\epsilon}}{\gamma\Delta} L_{22}\right]. \quad (47)$$

The various terms have the same meaning as defined in Eq. (28).

In view of the energy, Eq. (35), one can readily obtain the equation for pressure, i.e.,

$$P = P^{id} + P^{HB} + P^{t} + P^{Q}. \quad (48)$$

The equations for the different contributions to pressure can be straightforwardly obtained from the respective free energy as

$$\frac{\beta P}{\rho} = \rho \frac{\partial}{\partial \rho}\left(\frac{F}{NkT}\right). \quad (49)$$

We have used the inputs of Table I in these relations to compute G_{xs} for He-H_2 mixture as a function of He composition c_{He}, T, and P. The effect of temperature on G_{xs} is depicted in Fig. 2 for a given pressure P=0.5 GPa. G_{xs} is quite asymmetric around c_{He}=0.5, which is more pronounced at low temperatures. For example, at T=10K, G_{xs} is positive towards the H_2-rich side. As the composition of He in the mixture increases, G_{xs} becomes negative implying order and greater thermodynamic stability. The role of temperature on G_{xs} is more dominant towards the He-rich side. G_{xs} of the mixture increases considerably with increasing T for rich compositions of He.

The pressure effect on G_{xs} is shown in Figs. 3(a) and 3(b) for T=15 K and in Figs. 4(a) and 4(b) for T=100 K. The computed values of G_{xs} in the megapascal range (1.0 MPa, 5.0 MPa, and 10.0 MPa) and in the gigapascal range (0.1 GPa, 0.5 GPa, 1.0 GPa, and 2.0 GPa) of pressures are displayed. In the MPa range of pressures (T=15 K), G_{xs} is positive and increases with increasing P. However, in the GPa range of pressures, G_{xs} decreases with increasing pressures. G_{xs} also exhibits a crossover from positive values at

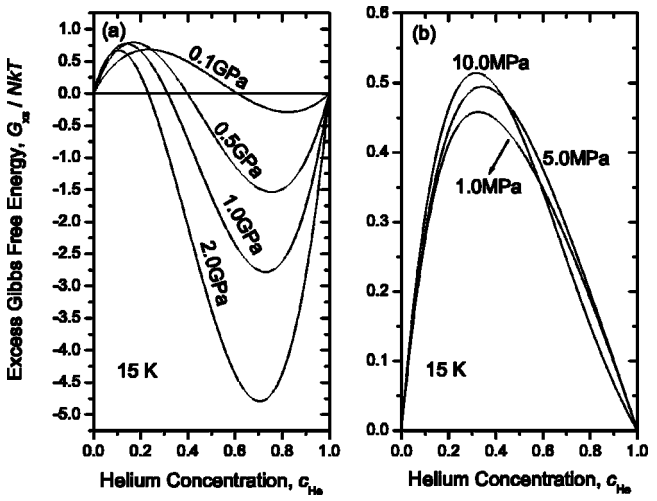

FIG. 3. Effect of pressure on G_{xs}/NkT at 15 K for He-H_2 mixture as a function of c_{He}: (a) gigapascal (GPa) range of pressures, (b) megapascal (MPa) range of pressures.

H_2-rich end to large negative values towards He-rich end for larger pressures of GPa range. The general trend of the effect of pressure at T=100 K is also similar, but the magnitude of G_{xs} at 100 K is much smaller than that at 15 K.

V. EXCESS ENTROPY OF MIXING

It is quite evident from the previous discussion that G_{xs} of the He-H_2 mixture depends strongly on temperature and, therefore, we have investigated the excess entropy which is a derivative of G_{xs} with respect to T. The excess entropy of mixing, S_{xs}, can be obtained from

$$S_{xs} = S - (c_1 S_1 + c_2 S_2) + Nk \sum c_i \ln c_i. \quad (50)$$

The various entropy terms on the right-hand side of the above equation are obtained by taking the temperature derivative of the different Gibbs free energy terms as they appear in Eq. (31),

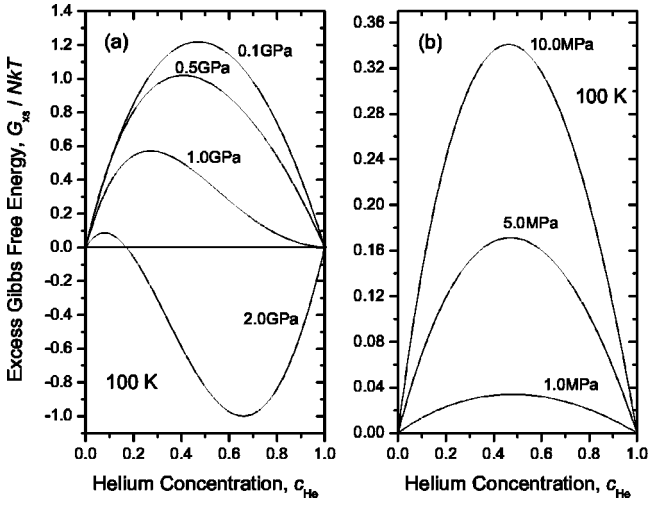

FIG. 4. G_{xs}/NkT as a function of c_{He} at T=100 K: (a) GPa range of pressures, (b) MPa range of pressures.

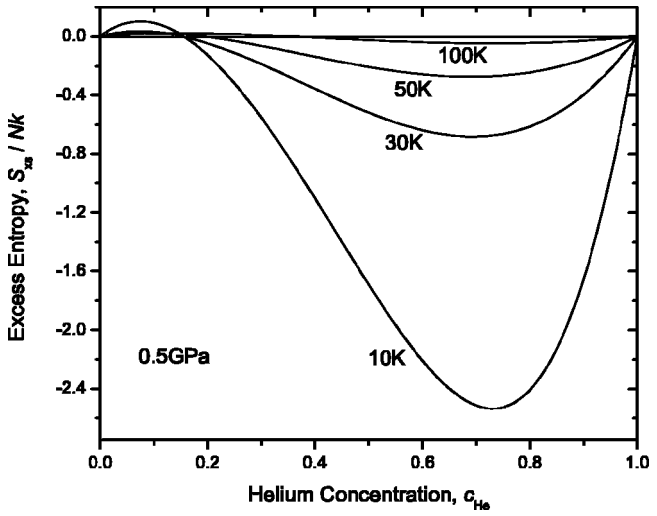

FIG. 5. Excess entropy of mixing (S_{xs}/Nk) for He-H_2 mixture as function of helium concentration c_{He} at 0.5 GPa for different temperatures, $T=10$ K, 30 K, 50 K, and 100 K.

$$S = -\left(\frac{\partial G}{\partial T}\right)_P = -\frac{\partial}{\partial T}(F^{\mathrm{id}} + F^{\mathrm{HB}} + F^{\mathrm{t}} + F^{\mathrm{Q}})_P + \frac{P}{\rho^2}\left(\frac{\partial \rho}{\partial T}\right)_P. \tag{51}$$

We may recall that the various F's and P's are functions of σ_{ij}, which in our scheme are T dependent [see Eq. (22)], and hence contribute to entropy. The temperature effect on S_{xs} is shown in Fig. 5 for a given $P=0.5$ GPa. S_{xs} is quite asymmetric and attains a lowest value towards the He-rich side. S_{xs} increases with increasing T. The impact of pressure on S_{xs} is shown in Fig. 6 for $T=15$ K and in Fig. 7 for $T=100$ K. The impact of MPa and GPa pressures on S_{xs} is quite different. As pressure increases from 1.0 MPa to 10.0 MPa ($T=15$ K) the asymmetry in S_{xs} shifts from the H_2-rich side to the He-rich side and, in addition, S_{xs} decreases with increasing pressure. At $T=100$ K, however, S_{xs} is small and positive in the MPa region and increases with increasing pressure. In the GPa range of pressures, S_{xs} exhibits strong asymmetry and changes from positive to negative values as the concentration of He increases.

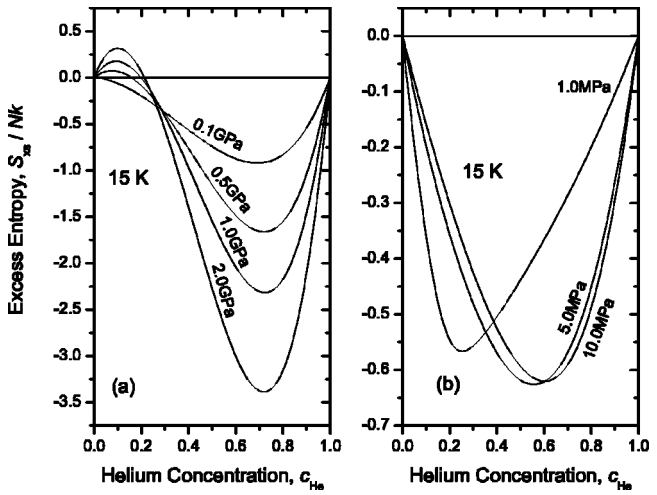

FIG. 6. S_{xs}/Nk as a function of c_{He} at $T=15$ K: (a) GPa range of pressures, (b) MPa range of pressures.

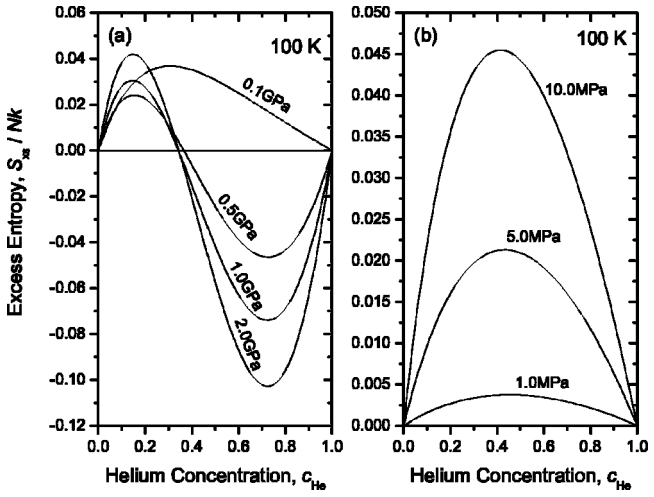

FIG. 7. S_{xs}/Nk as a function of c_{He} at $T=100$ K: (a) GPa range of pressures, (b) MPa range of pressures.

VI. CONCENTRATION FLUCTUATIONS AND THERMODYNAMIC STABILITY

The long wavelength limit $[q(=2\pi/\lambda)\to 0]$ of the concentration-concentration structure factor [28] $S_{cc}(0)$ provides valuable insight of the binary mixture at the atomic level (see, for example, Ref. [29]). $S_{cc}(0)$ is defined as

$$S_{cc}(0) = N\langle(\Delta c)^2\rangle, \tag{52}$$

where $\langle(\Delta c)^2\rangle$ represents the mean square fluctuations in the concentration. These can be derived from statistical mechanics in terms of the Gibbs free energy,

$$S_{cc}(0) = NkT\left(\frac{\partial^2 G}{\partial c_1^2}\right)^{-1}_{T,P,N}. \tag{53}$$

For an ideal mixture ($G=\Sigma_i c_i G_i^0 + NkT\Sigma_i c_i \ln c_i$) one simply obtains

$$S_{cc}^{\mathrm{id}} = c_1 c_2. \tag{54}$$

Any deviation of $S_{cc}(0)$ from the ideal values is of great interest to visualize the degree of order and the thermodynamic stability of the mixture. The significance of $S_{cc}(0)$ emerges due to the curvature $(\partial^2 G/\partial c_1^2)_{T,P,N}$, which undergoes a distinct transition at the extreme physicochemical conditions of the mixture. If, at a given composition, $S_{cc}(0) \gg S_{cc}^{\mathrm{id}}(0)$ then there is a tendency of segregation (like atoms tend to pair as nearest neighbors), or phase separation. On the other hand, $S_{cc}(0) \ll S_{cc}^{\mathrm{id}}(0)$ is an indication of heterocoordination (unlike atoms tend to pair as nearest neighbors). In the limiting cases, $S_{cc}(0)\to\infty$ for phase separation (demixing) and $S_{cc}\to 0$ for complete heterocoordination.

$S_{cc}(0)$ is directly related to the excess stability function E_{xs} originally introduced by Darken [30] to study the thermodynamic stability of mixtures,

$$E_{xs} = RT\left(\frac{1}{S_{cc}(0)} - \frac{1}{c_1 c_2}\right). \tag{55}$$

For a binary ideal mixture, $E_{xs}^{id}=0$.

One can also estimate from $S_{cc}(0)$ the Warren-Cowley [31,32] short range order parameter α_1, which helps to quantify the degree of segregation or heterocoordination. Phase separation is an extreme condition of segregation. By virtue of the basic thermodynamic relations, and taking the probabilistic approach, Bhatia and Singh [33] showed that the limiting values of α_1 lie in the range $-c_1/c_2 \leqslant \alpha_1 \leqslant 1$ for $c_1 < 0.5$ and $-c_2/c_1 \leqslant \alpha_1 \leqslant 1$ for $c_1 \geqslant 0.5$. Obviously, for equiatomic ($c_1=0.5$) binary mixture the limiting values tend to $-1 \leqslant \alpha_1 \leqslant 1$. For heterocoordination in the mixture, $\alpha_1 < 0$, with the minimum value of -1 rendering complete order of unlike pairs as nearest neighbors. For segregation, α_1 varies from 0 to +1, where $\alpha_1(\max)=1$ suggests total segregation, or phase separation.

For a mixture where size effects are relatively small, there exists (see Refs. [34,35]) an exact relation between $S_{cc}(0)$ and α_l for different shells,

$$\frac{S_{cc}(0)}{S_{cc}^{id}} = 1 + \sum_l z_l \alpha_l, \tag{56}$$

where z_l and α_l are the coordination number and the short range order (SRO) parameter for the lth shell (l varies from first neighbor shell to higher shells). For the nearest neighbor shell ($l=1$), Eq. (56) simplifies considerably to

$$\alpha_1 = \frac{S_{cc}^*(0) - 1}{(z-1)S_{cc}^*(0) + 1}, \tag{57}$$

where

$$S_{cc}^*(0) = \frac{S_{cc}(0)}{S_{cc}^{id}(0)}. \tag{58}$$

As stated earlier, one of the basic advantages of the present approach is that it allows us to study the effect of temperature and pressure on $S_{cc}^*(0)$, and, hence, on SRO parameter α_1. The nature of nearest neighbor pairs in the mixture, such as H_2-H_2, He-He, and He-H_2, can be readily inferred. The effect of T on $S_{cc}^*(0)$ is depicted in Fig. 8 at $P=0.5$ GPa. At low temperature ($T=10$ K) the mixture exhibits two important regions: (i) segregated [$S_{cc}^*(0)>1$, i.e., $\alpha_1>0$] region in the composition range $0 \leqslant c_{He} \leqslant 0.2$, where like atoms ($H_2$-$H_2$ and He-He) tend to be preferred as nearest neighbors and (ii) heterocoordinated [$S_{cc}^*(0)<1$, i.e., $\alpha_1<0$] region in the composition range $0.2 \leqslant c_{He} \leqslant 1$, where unlike atoms (He-H_2) tend to pair as nearest neighbors. With decreasing T, $S_{cc}^*(0)$ increases in the segregated region whereas it decreases in the heterocoordinated region. In the ordered phase of the mixture $S_{cc}^*(0)$ exhibits flat minima over a wide range of composition at $T \sim 10$ K.

The impact of pressure in the MPa range (1.0 MPa, 5.0 MPa, and 10.0 MPa) and GPa range (0.1 GPa, 0.5 GPa, and 1.0 GPa) at $T=15$ K is shown in Figs. 9(a) and 9(b), respectively. The effect of MPa and GPa pressures on $S_{cc}^*(0)$ in the segregation region is quite distinct. Even at low temperature ($T \sim 15$ K) the mixture exhibits a good deal of segregation over an extended region of composition for the MPa pressures. For the GPa pressures, however, the ordered phase dominates as the He concentration increases in the mixture. The results for $T=100$ K are shown in Fig. 10(a) for the MPa pressures and Fig. 10(b) for the GPa pressures. For the MPa pressures, $S_{cc}^*(0)>1(\alpha_1>0)$, i.e., segregation, at all compositions, which increases with increasing pressure from 1.0 MPa to 10.0 MPa. But, in the GPa range of pressures, the mixture transforms from segregation to ordered phase with increasing pressure.

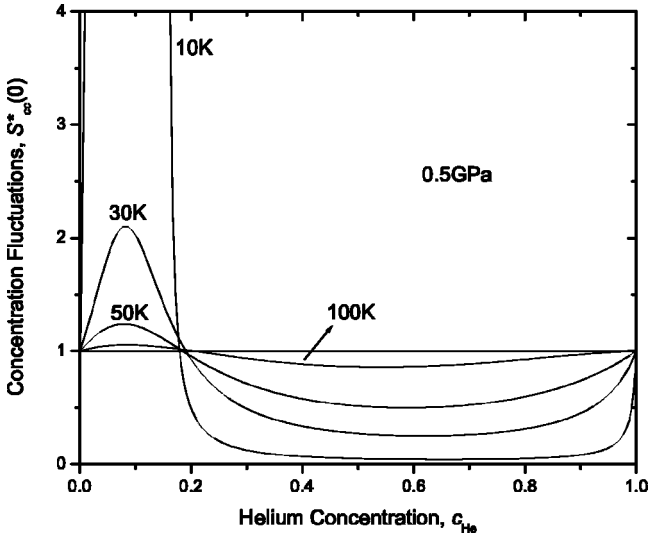

FIG. 8. Effect of temperature ($T=10$ K, 30 K, 50 K, and 100 K) on concentration fluctuations in the long wavelength limit [$S_{cc}^*(0) = S_{cc}(0)/S_{cc}^{id}(0)$] for He-$H_2$ mixture as a function of helium composition c_{He} at $P=0.5$ GPa.

VII. SUMMARY AND CONCLUSIONS

A theory of mixtures is developed on the basis of statistical mechanical perturbation scheme to study the compress-

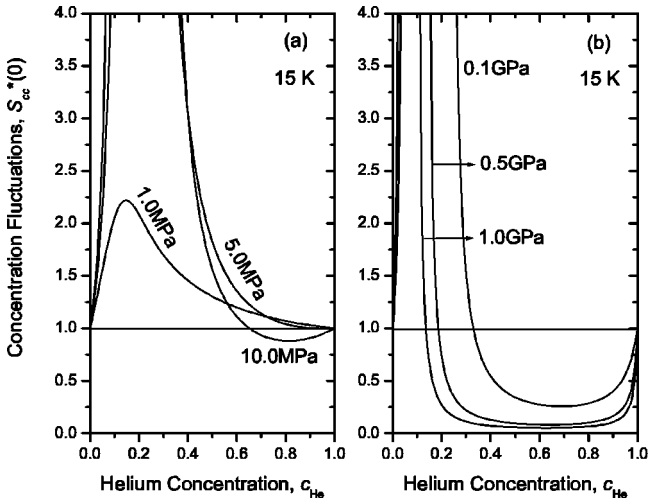

FIG. 9. $S_{cc}^*(0)$ for He-H_2 mixture as a function of c_{He} at $T=15$ K: (a) MPa range of pressures, (b) GPa range of pressures.

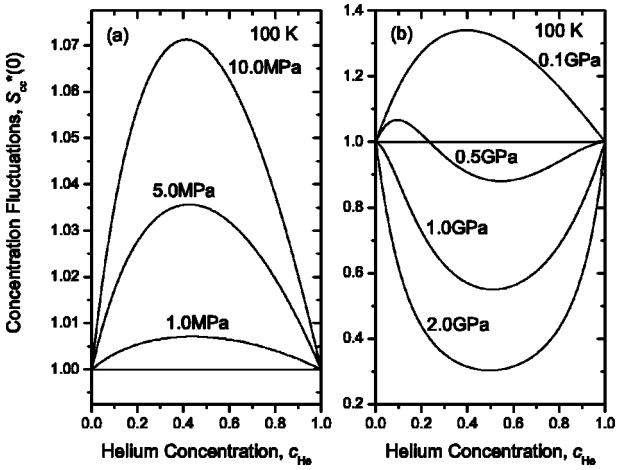

FIG. 10. $S_{cc}^*(0)$ for He-H_2 mixture as a function of c_{He} at $T=100$ K: (a) MPa range of pressures, (b) GPa range of pressures.

ibility factor Z, excess free energy of mixing G_{xs}, excess entropy S_{xs} of mixing, and the long wavelength limit of the concentration fluctuations $[S_{cc}(0)]$ of He-H_2 mixture over a wide range of pressure and temperature. He-H_2 mixtures enjoy special significance due to their cosmological relevance and the challenge they pose due to the complex nature of interactions among the constituent species. The long range correlations among the mixture species have been included through the double Yukawa potential, which acts as a perturbation to the hard sphere reference mixture. The dimerization of the H_2 molecule is accounted for as a hard sphere convex body fluid for which an equation of state can be derived based on the scaled particle theory.

Taking into account the quantum energy term and the contributions from long range correlations, an analytical expression for the equation of state of He-H_2 system is presented. This, in turn, is used to obtain the Helmholtz free energy, entropy, and $S_{cc}(0)$. At a given T, the equation of state has been solved numerically to give density as a function of pressure enabling us to express Z, G_{xs}, S_{xs}, and $S_{cc}(0)$ as functions of pressure. As a result, internal consistency of the various thermodynamic functions has been ensured.

The values of Z, G_{xs}, S_{xs}, and $S_{cc}(0)$ computed for He -H_2 as functions of composition at different P and T are given. The parameters of the double Yukawa potential are simulated to the exp-6 potential, which conforms satisfactorily to the *ab initio* quantum mechanical calculations of He and H_2 energy data. The role of the various components of Z and its dependence on the radial distribution function at low and high density regions have been critically examined. The characteristic behaviors of G_{xs}, S_{xs}, and $S_{cc}(0)$ have been studied both in the MPa and GPa ranges of pressures with a view to investigate the segregation and heterocoordination for thermodynamic stability in the mixture. Some of the important conclusions of the present work are as follows.

(a) The contributions from the long range correlations Z^t and the quantum correction term Z^Q to the compressibility factor Z are quite dominant at low temperatures. Similarly, the impact of the distribution function on Z is quite substantial at low temperatures. The dilute limit $[g(r)=1]$ is only valid at high temperatures.

(b) The computed values of pressure agree very well with computer simulation results over an extended region of temperature (50 K–4000 K) and pressure (0.05 GPa–16 GPa).

(c) Segregation, heterocoordination, or both may occur in the He-H_2 mixture depending upon its composition, temperature, and pressure.

(d) Though the results from all the three thermodynamic functions [G_{xs}, S_{xs}, and $S_{cc}(0)$] are consistent, $S_{cc}(0)$ is most useful and sensitive to study the phase separation or chemical order in the mixture.

At low temperature, $T=15$ K, segregation occurs for the MPa pressures (1.0 MPa, 5.0 MPa, and 10.0 MPa), which increases with increasing pressures. For the GPa range (0.1 GPa, 0.5 GPa, 1.0 GPa, and 2.0 GPa), heterocoordination (order) prevails, which increases as the composition of He increases. At $T=100$ K, however, there is a noticeable increase of segregation with increasing MPa pressures. As the pressure tends to the GPa range, a reversal of the trend is observed. The mixture transforms from segregation to ordered phase with increasing GPa pressures.

ACKNOWLEDGMENT

This work was supported by the Sultan Qaboos University, Grant No. IG/SCI/PHYS/01/03.

[1] J. A. Schouten, Phys. Rep. **172**, 33 (1989).
[2] N. H. March, *Liquid Metals-Concepts and Theory* (Cambridge University Press, Cambridge, 1990), p. 325.
[3] W. B. Street, Astrophys. J. **186**, 1107 (1973).
[4] D. J. Klein and N. H. March, Phys. Chem. Liq. **28**, 207 (1994).
[5] Francis H. Ree, J. Chem. Phys. **78**, 409 (1983).
[6] L. C. van den Bergh and J. A. Schouten, J. Chem. Phys. **89**, 2236 (1988).
[7] P. J. Leonard, D. Henderson, and J. A. Barker, Mol. Phys. **21**, 107 (1971).
[8] E. W. Grundke, D. Henderson, J. A. Barker, and P. J. Leonard, Mol. Phys. **25**, 883 (1973).
[9] D. Henderson, Annu. Rev. Phys. Chem. **25**, 461 (1974).
[10] G. M. Torrie and J. P. Valleau, J. Chem. Phys. **66**, 1402 (1977).
[11] S. M. Foiles and N. W. Ashcroft, J. Chem. Phys. **75**, 3594 (1981).
[12] D. J. Gonzalez and M. Silbert, J. Phys. C **16**, 1097 (1983).
[13] A. Garcia and D. J. Gonzalez, Phys. Chem. Liq. **18**, 91 (1988).
[14] E. P. Wigner, Phys. Rev. **40**, 749 (1932).
[15] J. G. Kirkwood, Phys. Rev. **44**, 749 (1933).
[16] R. M. Gibbons, Mol. Phys. **18**, 809 (1970).
[17] J. Largo and J. R. Solana, Phys. Rev. E **58**, 2251 (1998); Mol.

Phys. **96**, 1367 (1999).
[18] S. M. Osman and R. N. Singh, Phys. Rev. E **51**, 332 (1995).
[19] S. M. Osman and R. N. Singh, Mol. Phys. **96**, 87 (1999).
[20] T. Boublik, J. Chem. Phys. **53**, 471 (1970).
[21] G. A. Mansoori, N. F. Carnahan, K. E. Starling, and T. W. Leland, J. Chem. Phys. **54**, 1523 (1971).
[22] C. Barrio and J. R. Solana, J. Chem. Phys. **113**, 10 180 (2000).
[23] N. F. Carnahan and K. E. Starling, J. Chem. Phys. **51**, 635 (1969).
[24] C. Barrio and J. R. Solana, Mol. Phys. **94**, 809 (1998).
[25] D. H. L. Yau, K.-Y. Chan, and D. Henderson, Mol. Phys. **91**, 1137 (1997).
[26] D. Henderson and K.-Y. Chan, Mol. Phys. **94**, 253 (1998).
[27] Y. Tang and Benjamin C-Y. Lu, J. Chem. Phys. **103**, 7463 (1995).
[28] A. B. Bhatia and D. E. Thornton, Phys. Rev. B **2**, 3004 (1970).
[29] R. N. Singh and F. Sommer, Rep. Prog. Phys. **60**, 57 (1997).
[30] L. S. Darken, Trans. Metall. Soc. AIME **80**, 239 (1967).
[31] B. E. Warren, *X-Ray Diffraction* (Addison Wesley, Reading, MA, 1969).
[32] J. M. Cowley, Phys. Rev. **77**, 667 (1950).
[33] A. B. Bhatia and R. N. Singh, Phys. Chem. Liq. **11**, 285 (1982).
[34] H. Ruppersberg and H. Egger, J. Chem. Phys. **63**, 4095 (1975).
[35] N. H. March, S. Wilkins, and J. E. Tibbals, Cryst. Lattice Defects **6**, 253 (1976).